Springer

Acta Mechanica Sinica

CrossMark click for updates

• RESEARCH PAPER •

Acta Mech. Sin., Vol. 41, 524456 (2025)
https://doi.org/10.1007/s10409-024-24456-x

Efficient obstacle avoidance planning for multi-robot suspension system based on a collaborative optimization for force and position

Xiangtang Zhao[1,2], Zhigang Zhao[1,2*], Cheng Su[1], Jiadong Meng[1,2], and Hutang Sang[1]

[1] *School of Mechanical Engineering, Lanzhou Jiaotong University, Lanzhou 730070, China;*
[2] *State Key Laboratory of Rail Transit Vehicle System, Southwest Jiaotong University, Chengdu 610031, China*

Received August 28, 2024; accepted November 8, 2024; published online January 14, 2025

To avoid collisions between a suspended object, cables, towing robots, and obstacles in the environment in a multi-robot suspension system, obstacle avoidance planning was studied based on a collaborative optimization method for force and position. Based on the analysis of the kinematics and dynamics of the system, the inverse kinematics and inverse dynamics of the system are solved using the least variance method. The obstacle avoidance planning is performed in the solved collision-free feasible space using the stable dung beetle optimization (SDBO) algorithm, which ensures that the suspended object can move stably to the target point in the workspace. The optimal obstacle avoidance trajectory of the multi-robot suspension system can be accurately determined by using the collaborative optimization method for force and position to plan the towing robot and the cable. Finally, the correctness of the obstacle avoidance planning method is verified by simulations. By taking a special scenario, the remarkable findings reveal that the SDBO algorithm outperforms the dung beetle optimization algorithm by reducing the length of the planned trajectory of the suspended object by 14.51% and the height by 79.88%, and reducing the minimum fitness by 95.84% and the average fitness by 94.77%. The results can help the multi-robot suspension system to perform various towing tasks safely and stably, and extend the related planning and control theory.

Suspension system, Obstacle avoidance planning, Collision-free feasible space, Stable dung beetle optimization, Collaborative optimization for force and position

Citation: X. Zhao, Z. Zhao, C. Su, J. Meng, and H. Sang, Efficient obstacle avoidance planning for multi-robot suspension system based on a collaborative optimization for force and position, Acta Mech. Sin. 41, 524456 (2025), https://doi.org/10.1007/s10409-024-24456-x

1. Introduction

Due to the demand for applications in the civil, industrial, and military sectors, suspension systems have gradually evolved from single operations to cluster operations. In practice, it is also necessary for several robots to work together to process the same object, such as the handling of large equipment, the transportation of heavy goods, or the operation tasks on special occasions. Therefore, the multi-robot suspension system consisting of traction robots working in parallel was studied. Such a system is essentially characterized by high traction capacity, large workspace, and flexibility [1,2]. At present, a multi-robot coordinated suspension system for towing large-volume and high-mass objects mainly relies on the operator to perform the towing task based on experience or continuous trials in practice and lacks scientific theoretical, and technical guidance. Therefore, a comprehensive theoretical study for such a multi-robot suspension system is urgently needed to support practical operation [3,4]. Due to the flexibility and one-way tension characteristics of the cable, the swing of the suspended object and wrap of the cables may occur, which will affect the stability and safety of the system. Therefore, it is necessary to investigate the planning and optimization methods for such systems.

At present, related research on multi-robot suspension systems has just begun at home and abroad, but the research results of cable-driven parallel robots provide some valuable reference for the research of multi-robot suspension systems

*Corresponding author. E-mail address: zhaozhg@mail.lzjtu.cn (Zhigang Zhao)
Executive Editor: Qiang Tian

[5,6]. For the multi-robot suspension system in the air, Mohammadi et al. [7-9] used the Lyapunov function to avoid collisions between UAVs, and the advantage is that the controller does not need to solve the tension of the cable. Maza et al. [10] and Kondak et al. [11] used three small UAVs to conduct towing experiments and mainly studied the modeling method of the three UAVs and the control of the suspended object. Michael et al. [12] and Jiang and Kumar [13] modeled the suspension system of several UAVs and studied the vibration and static stability of the suspended object. Another research direction is the cooperative towing of objects by multiple ground robots. Xiang et al. [14], Kamadaet et al. [15], and Cote et al. [16] studied the force distribution of the cable in the cable-driven mechanism and proposed to optimize the force distribution of the mechanism with the P-norm. Yamamoto et al. [17] discussed the characteristics of the unconstrained suspension mechanism and performed an inverse dynamic analysis of the suspension mechanism. Su et al. [18,19] established the model of the coordinated multi-robot suspension system and analyzed the workspace of the system. Existing research on multi-robot suspension systems has primarily focused on the kinematics, dynamics, workspace, and stability, which have yielded promising results. Due to the coupled and nonlinear characteristics of the system, the multiple solutions for the kinematics of a multi-robot coordinated suspension system make motion planning a multi-layer optimization problem. To ensure the effective and controllable movement of suspended objects in a multi-robot coordinated suspension system, accurate planning of the movement of suspended objects in the workspace is essential.

Obviously, there are numerous results on trajectory planning for cable-driven parallel robots and multiple UAVs. However, little research has been done on obstacle avoidance planning for a coordinated suspension system with multiple robots. Zhu et al. [20] proposed an optimization method for the motion planning of robots in a dynamic environment, where each robot must make accurate motion predictions for the neighboring robots to avoid collisions. Zhao et al. [21] discussed obstacle avoidance and point-to-point planning of suspended objects by multiple cranes, but the obstacle avoidance of the cables was ignored. Lin et al. [22] searched for the globally optimal path based on the path planning algorithm of the grid method for the towing operation, however, this method is not suitable for obstacle avoidance in three dimensions. In general, the trajectory planning for a multi-robot suspension system mainly focuses on obstacle avoidance planning for suspended objects, which is similar to the traditional planning for a single rigid body. However, the multi-robot suspension system consists of multiple robots attached to the same object with cables, which is a tightly coupled three-dimensional multi-vector and multi-rigid body system. It is therefore necessary to discuss the obstacle avoidance planning of the suspended object, cables, towing robots, and obstacles with each other in space.

The intelligent planning algorithm has strong compatibility with the environment and is capable of optimizing trajectories and avoiding obstacles according to the information obtained in the planning process in real-time. Common static trajectory planning methods include ant colony optimization (ACO) [23], genetic algorithm (GA) [24], and particle swarm optimization (PSO) [25] among others. Although group intelligence algorithms have a good trajectory planning ability, it is difficult for these algorithms to achieve quality trajectories in a short time in a complex environment, so it is commonly suggested to utilize improved group intelligence algorithms for robot trajectory planning. Qian et al. [26] applied an improved ant colony algorithm to enhance the quality of obstacle avoidance paths for suspended objects, albeit without considering the coordination and consistency of kinematics and dynamics of the system. Mishra et al. [27] used the GA to optimize the objective function to obtain the shortest path in the joint space of the cable-driven parallel robot. Zhen et al. [28] proposed an intelligent self-organization algorithm to solve the collaborative task planning of multiple UAVs, the global optimization is decomposed into a local optimization for a single UAV. Li et al. [29] created a three-dimensional environment model for the suspension of aerial robots and realized the planning of the shortest path using an ant colony algorithm, but did not consider force planning. Fu et al. [30] proposed a multi-UAV collaborative trajectory planning method based on the modified cheetah optimization algorithm. Shen et al. [31] proposed a multi-strategy dung beetle optimizer for UAV path planning, which balances exploration and development capabilities. The above-improved algorithm was capable of optimizing the trajectory planning problem, but it does not fully solve the trajectory planning requirements in the obstacle environment. The dung beetle optimization (DBO) algorithm [32] divided different tasks according to the difference of labor and considered both global exploration and local development, which can solve the shortest trajectory problem of the known static environment more efficiently and quickly. At the same time, the DBO algorithm has been widely employed in robot trajectory planning due to its good compatibility and easy of combining with other algorithms and strategies.

According to the spatial configuration, the multi-robot suspension system is a tightly coupled system with rigid vectors, and obstacle avoidance planning can not be performed by the obstacle avoidance planning method of a single particle. Moreover, the force space of the cable and the position space of the suspended object are highly coincident, resulting in a strong correlation between motion planning and force planning. With regard to these scientific

gaps, the present research is conducted on obstacle avoidance planning for a multi-robot suspension system using a collaborative optimization approach. The main contributions of this study can be outlined as follows:

(1) In a coordinated suspension system with multiple robots, the variable position of the suspended object affects the tension of the cable, that is, the position space and force space of the system are coincident, so force planning is required when planning obstacle avoidance. The overall obstacle avoidance planning scheme is given in terms of the coupling characteristics of the system.

(2) Making enhancements to the DBO algorithm to boost search performance and trajectory planning efficiency. These mainly include: the use of a reverse learning strategy for population initialization, a sine-cosine strategy for temporary population establishment, an optimal individual variation strategy for global optimal solution mutation, and the introduction of a stability constraint factor for trajectory planning safety.

(3) The stable dung beetle optimization (SDBO) algorithm is used to perform obstacle avoidance planning for a suspended object, meanwhile, by adjusting the length and tension of the cable, the obstacle avoidance of the cable and the towing robot is realized. The objective function is constructed by multiple performance metrics, and the optimal trajectory of the suspension system is obtained based on the collaborative optimization method for force and position.

The subsequent sections of this paper are organized in the following form. In Sect. 2, the kinematic and dynamic models of the system are established, and principles of the DBO algorithm are introduced. In Sect. 3, an obstacle avoidance planning method for a multi-robot suspension system is proposed based on an improved DBO algorithm and a collaborative optimization method for force and position. In Sect. 4, simulation experiments on obstacle avoidance planning are performed, and the results are compared with those of other algorithms. Finally, some noticeable results and concluding remarks are presented in Sect. 5.

2. Preliminaries

2.1 Problem formulation

In the process of industrial manufacturing, building construction, or assembly of large machinery, it is often necessary to carry equipment or components with large weight and huge size. Three robots can work together to tow the heavy equipment from one location to another, ensuring the safety and efficiency of the towing process. The spatial configuration of the suspension system designed for the transport of heavy objects in the industry is illustrated in Fig. 1. The towing robot consists of a fixed base and a 3-

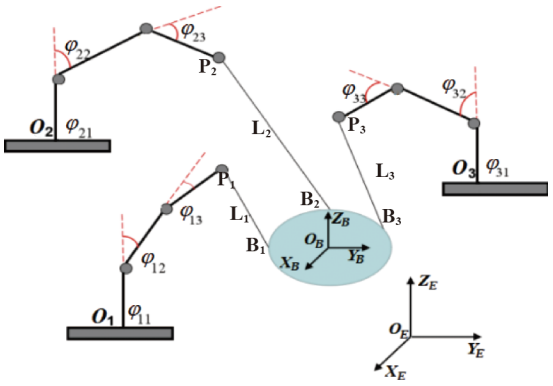

Figure 1 Spatial configuration of the suspension system.

DOF joint robot, the rod length of the robot is mathematically represented by (a_{k1}, a_{k2}, a_{k3}), the joint angle by $(\varphi_{k1}, \varphi_{k2}, \varphi_{k3})$, and the position vector of the cable by $\mathbf{L}_k$. According to the spatial structure of the suspension system, the following coordinate systems are established. The inertial coordinate system $\{O_E\}$ is established at a point on the horizontal plane, the coordinate system $\{O_i\}$ is established at the bottom of the robot, and the coordinate system $\{O_B\}$ is established at the barycenter of the suspended object. The position of the connection point between the end of the robot and the cable is $\mathbf{P}_k$, the position of the connection point between the cable and the suspended object is $\mathbf{B}_k$, and the position and posture of the suspended object are (x, y, z, a_1, a_2, a_3). Since the entire system consists of three towed robots, their relationship can be expressed as $k = 1, 2, 3$.

Due to the physical connection between the towing robot, the cable, and the suspended object, so the system is tightly coupled. Obstacle avoidance planning should consider not only the suspended object but also the planning with multiple rigid bodies and multiple vectors. Therefore, obstacle avoidance planning for a suspension system can be defined as planning with multiple rigid bodies and multiple vectors with a collaborative optimization method for force and position. The obstacle avoidance planning method for suspension systems is discussed. The tension of the suspension system can be reasonably distributed automatically through scientific and rational motion planning of the system, which can effectively improve the smoothness and stability of the towing operation of the multi-robot coordinated suspension system.

Depending on the drive type of suspension system, the multi-robot coordinated suspension system can be divided into four categories [18]: the cable-driven multi-robot suspension system, the end-driven multi-robot suspension system, the base-driven multi-robot suspension system, and the hybrid-driven multi-robot suspension system. In this paper, the obstacle avoidance planning method for a cable-driven multi-robot coordinated suspension system, where

the end position of the towing robot is fixed and the position of the suspended object can only be changed by adjusting the cable length, is discussed.

2.2 Kinematic analysis

When the towing robot is not pulled by the cable, the end position $\mathbf{P}_k(x_{Pk}, y_{Pk}, z_{Pk})$ of the robot is solved using the D-H transformation in $\{O_k\}$ as follows:

$$\begin{bmatrix} x_{pk} \\ y_{pk} \\ z_{pk} \end{bmatrix} = \begin{bmatrix} a_{k2}\cos\varphi_{k1}\sin\varphi_{k2} + a_{k3}\cos\varphi_{k1}\sin(\varphi_{k2}+\varphi_{k3}) \\ a_{k2}\sin\varphi_{k1}\sin\varphi_{k2} + a_{k3}\sin\varphi_{k1}\sin(\varphi_{k2}+\varphi_{k3}) \\ a_{k1} + a_{k2}\cos\varphi_{k2} + a_{k3}\cos(\varphi_{k2}+\varphi_{k3}) \end{bmatrix}. \tag{1}$$

When the cable is tensioned, it is treated as a rigid body, and its elastic deformation and mass are neglected. The kinematic equations for the suspension system are as follows [33]:

$$\mathbf{L}_k = \mathbf{P}_k - \mathbf{B}_k = \mathbf{P}_k - \mathbf{R}\mathbf{B}'_k - \mathbf{H}, \tag{2}$$

$$L_k = \sqrt{(\mathbf{P}_k - \mathbf{B}_k)^{\mathrm{T}}(\mathbf{P}_k - \mathbf{B}_k)}, \tag{3}$$

where $\mathbf{H} = [x \quad y \quad z]^{\mathrm{T}}$ denotes the centroid position of the suspended object, $\mathbf{B}'_k$ signifies the connecting position between the suspended object and the cable in the coordinate system $\{O_B\}$, $\mathbf{R}$ stands for the transformation matrix of the $\{O_B\}$ with respect to $\{O_E\}$.

$$\mathbf{R} = \mathbf{R}_z(\alpha_3)\mathbf{R}_y(\alpha_2)\mathbf{R}_x(\alpha_1) = \begin{bmatrix} \cos\alpha_2\cos\alpha_3 & \sin\alpha_1\sin\alpha_2\cos\alpha_3 - \sin\alpha_3\cos\alpha_1 & \sin\alpha_2\cos\alpha_1\cos\alpha_3 + \sin\alpha_1\sin\alpha_3 \\ \sin\alpha_3\cos\alpha_2 & \sin\alpha_1\sin\alpha_2\sin\alpha_3 + \cos\alpha_1\cos\alpha_3 & \sin\alpha_2\sin\alpha_3\cos\alpha_1 - \sin\alpha_1\cos\alpha_3 \\ -\sin\alpha_2 & \sin\alpha_1\cos\alpha_2 & \cos\alpha_1\cos\alpha_2 \end{bmatrix}.$$

When the suspended object moves according to the desired trajectory, the end position of the robot and the length of the cable are adjusted accordingly, and these changes have a variety of cases, namely, the inverse kinematics of the suspension system has multiple solutions. The results of the analysis show that the position of the suspended object in the workspace corresponds to several feasible combinations of the end position of the towing robot and the length of the cable. In practice, an optimal combination should be chosen taking into account certain constraints. In some cases, one of the cables in the system may fail under other tensions, at that time, it is necessary to combine the dynamics of the suspension system to determine whether the tension of the cable is greater than zero.

2.3 Dynamic analysis

The force balance equation is often used to describe the relationship between the external force on an object and its state of motion, which is crucial for planning and controlling the motion of the suspended object. The balance equation of the suspended object is stated by [34]

$$\mathbf{J}^{\mathrm{T}}\mathbf{T} = \mathbf{F}, \tag{4}$$

where $\mathbf{T} = \begin{bmatrix} T_1 & T_2 & T_3 \end{bmatrix}^{\mathrm{T}}$ represents the tension of the cable such that $\mathbf{T}_{\min} \leqslant \mathbf{T}_k \leqslant \mathbf{T}_{\max}$, the size of matrix $\mathbf{T}$ is 3×1. And $\mathbf{J}^{\mathrm{T}} = \begin{bmatrix} \mathbf{J}_1 & \mathbf{J}_2 & \mathbf{J}_3 \end{bmatrix}$ denotes the structural matrix of the suspension system, the size of matrix $\mathbf{J}^{\mathrm{T}}$ is 6×3, whose components are expressed by

$$\mathbf{J}_k = \begin{bmatrix} \mathbf{u}_k \\ \left(\mathbf{R}\mathbf{B}'_k\right) \times \mathbf{u}_k \end{bmatrix}, \tag{5}$$

where $\mathbf{u}_k = \mathbf{L}_k / \| \mathbf{L}_k \|$ is the unit length vector of the cable.

In addition, $\mathbf{F}$ signifies the external force and torque acting on the suspended object in Eq. (4), the size of matrix $\mathbf{F}$ is 6×1, and can be formulated as

$$\mathbf{F} = \left[(m\ddot{x},\ m\ddot{y},\ m\ddot{z} + mg)^{\mathrm{T}},\ (I_x \cdot \ddot{\alpha}_1,\ I_x \cdot \ddot{\alpha}_2,\ I_z \cdot \ddot{\alpha}_3)^{\mathrm{T}}\right], \tag{6}$$

where m, $\left(I_x, I_y, I_z\right)$, $(\ddot{x}, \ddot{y}, \ddot{z})$, and $(\ddot{\alpha}_1, \ddot{\alpha}_2, \ddot{\alpha}_3)$ in order are the mass, the moment of inertia, the translational acceleration, and angular acceleration of the suspended object, respectively.

The inverse kinematics of multi-robot suspension system refers to the solution of the end position of each towing robot, cable tension, and cable length given the expected trajectory of the suspended object [35]. In the absence of constraints, the kinematic and dynamic equations of the system, namely Eqs. (2) and (4), yield a total of nine sub-equations and involve a total of fifteen unknowns, the unknown variables include nine end positions, three cable tension, and three cable length. The number of unknowns is larger than the number of established equations, and the suspension system has multiple solutions. Consequently, direct determination of the tension $\mathbf{T}_k$, the length l_k of the cable, and the end position $\mathbf{P}_k$ of the robot is infeasible. To make the inverse solution of the suspension system exist, kinematic and dynamic equations of the suspension system should be simultaneously solved, and the tension of each cable should be guaranteed to be positive. However, the structure matrix of the suspension system is not a square matrix, and the cable tension can not be obtained from the null space matrix $\mathbf{N}(\mathbf{J}^{\mathrm{T}})$ of the structure matrix. According to the principle of vector closure, the gravity and inertia forces of the suspended object can be regarded as virtual cable

forces, and the virtual cable provides tension for the suspended object [36]. Therefore, the tension of the cable needs to be calculated through the generalized inverse of the matrix, then the tension of the cable is given by

$$\mathbf{T} = \mathbf{T}_s + \mathbf{T}_n = \mathbf{J}^{+}\mathbf{F} + \boldsymbol{\delta} \cdot \mathbf{N}(\mathbf{J}^{\mathrm{T}}), \tag{7}$$

where $\mathbf{J}^{+} = \mathbf{J}^{\mathrm{T}}(\mathbf{J}\mathbf{J}^{\mathrm{T}})^{-1}$ represents the generalized inverse matrix of the structure matrix $\mathbf{J}^{\mathrm{T}}$, $\boldsymbol{\delta}$ denotes any two-dimensional vector, $\mathbf{N}(\mathbf{J}^{\mathrm{T}})$ is the null space vector of the structure matrix $\mathbf{J}^{\mathrm{T}}$, $\mathbf{T}_s$ represents the unique special solution of Eq. (4), $\mathbf{T}_n$ stands for the general solution of Eq. (4), which does not work for the system but can change the tension distribution of the cable.

2.4 Principles of the DBO algorithm

The DBO algorithm is inspired by the natural behaviors of the dung beetles, which include ball-rolling, dancing, foraging, stealing, and reproduction [37]. By simulating the natural behavior of the dung beetles, the algorithm updates the position of the solution to find the optimal solution of the objective function. The objective function is usually defined according to the requirements of the optimization problem. The population is divided into proportionally different roles, the population size of the dung beetles is set at 30, and the numbers of the ball-rolling and dancing dung beetles, the spawning dung beetles, the foraging dung beetles, and the stealing dung beetles are 6, 6, 7, and 11, respectively.

The DBO algorithm is implemented with different position update strategies to simulate the search strategy of the dung beetles in the natural environment. The DBO algorithm includes the following update strategies:

(1) Ball-rolling behavior: to simulate the behavior of dung beetles rolling dung balls, the position update equation is as follows:

$$X_{ij}^{iter+1} = X_{ij}^{iter} + \sigma \cdot \varsigma \cdot X_{ij}^{iter-1} + \xi \cdot \Phi, \tag{8}$$

where *iter* represents the current iteration number, X_{ij}^{iter} refers to the position information of the *i*-th dung beetle in the *j*-th dimension in the *iter*-th iteration, σ is a natural coefficient, ς is a deflection coefficient, ξ is a constant, Φ simulates changes in light intensity.

(2) Dancing behavior: when dung beetle encounters obstacles, it adjusts its direction by dancing. The position update equation is as follows:

$$X_{ij}^{iter+1} = X_{ij}^{iter} + \tan(\theta)\left|X_{ij}^{iter} - X_{ij}^{iter-1}\right|, \tag{9}$$

where $\theta \in [0,\pi]$, if θ is equal to 0, $\pi/2$, or π, the dung beetle's position will not be updated. This avoids mathematical singularity in the updating process and ensures the stability of the algorithm. The values of θ are randomly generated within [0, π] by a uniformly distributed to simulate the behavior of dung beetles that randomly change direction in a natural environment.

(3) Spawning behavior: the renewal of the spawning area of the female dung beetles is simulated, and the dung beetle's position within the area will be updated. The position update equation is as follows:

$$X_{ij}^{iter+1} = X^{*} + \mathbf{b}_1 \cdot \left(X_{ij}^{iter} - Lb^{*}\right) + \mathbf{b}_2 \cdot \left(X_{ij}^{iter} - Ub^{*}\right), \tag{10}$$

where X^{*} represents the current local optimal position, b_1 and b_2 are two independent random vectors, Lb^{*} and Ub^{*} represent the lower and upper boundaries of the spawning area, respectively.

(4) Foraging behavior: the behavior of the dung beetles in the optimal foraging area is simulated, the position update equation is as follows:

$$X_{ij}^{iter+1} = X_{ij}^{iter} + C_1 \cdot \left(X_{ij}^{iter} - Lb^{\times}\right) + C_2 \cdot \left(X_{ij}^{iter} - Ub^{\times}\right), \tag{11}$$

where C_1 represents a random number following a normal distribution, C_2 represents a random vector in the range (0,1), $Lb^{\times}$ and $Ub^{\times}$ are the lower and upper boundaries of the optimal foraging area, respectively.

(5) Stealing behavior: the stealing behavior of dung balls between dung beetles is simulated, the position update equation is as follows:

$$X_{ij}^{iter+1} = X^{b} + Q \cdot \mathbf{h} \cdot \left(\left|X_{ij}^{iter} - X^{*}\right| + \left|X_{ij}^{iter} - X^{b}\right|\right), \tag{12}$$

where X^{b} is the best food source, $\mathbf{h}$ is a random vector of normal distribution, Q is a constant.

The DBO algorithm can achieve fast convergence and high accuracy by balancing global exploration and local development with different position update strategies. During the implementation of the DBO algorithm, the algorithm will evaluate the fitness of each dung beetle position based on the objective function and update the dung beetle position based on the fitness. The implementation steps of the DBO algorithm typically consist of initializing the population, evaluating the fitness, updating the positions and directions, iteratively updating until the termination condition is satisfied, and finally outputting the optimal solution.

3. Methods

3.1 Architecture

The structure of a multi-robot suspension system leads to the force space and position space overlap, the suspended object is connected to each robot by a cable, and the different positions of the suspended object correspond to the different end positions of the towing robot and the length of the cable. Therefore, the planning of a multi-robot coordinated suspension system should systematically consider not only the

trajectory planning of the suspended object, but also the elements of the end position of the towing robot, the length, and the tension of the cable. When there are multiple solutions in the system, it is necessary to optimize the multiple solutions to achieve a smooth trajectory. When different towing robots have the same position, the solution should be discarded to avoid collisions among the towing robots. At the same time, it is necessary to discard solutions that may cause interference with the cables.

When the cable of the suspension system is in a tension state during the towing process, the cable can be seen as a rigid vector, and the suspended object, cables, and towing robots can be seen as multiple rigid bodies. According to the coupling properties of the system, the suspended object and the cable have to be planned simultaneously. Multiple performance indexes are synthesized, the optimal position of the suspended object is achieved by an intelligent optimization algorithm, and the desired trajectory is obtained by interpolation. At the same time, considering the characteristics of the cable vector, the method of the collaborative optimization method for force and position is used to optimize the end trajectory of the towing robot and realize the obstacle avoidance of the cable, the optimal motion trajectory of the towing robot, length, and tension of the cable is obtained.

In summary, the overall scheme of obstacle avoidance planning for a multi-robot suspension system is shown in Fig. 2. The detailed steps are as follows:

(1) The optimal model of the multi-robot suspension system is obtained by simplifying the environmental obstacles and the system structure in three-dimensional space. Then, the collision-free feasible space of the system is calculated by using convex optimization algorithms and semi-definite programming (SDP) in the suspension environment.

(2) Considering the kinematic and dynamic constraints of the towing robots, the objective function is constructed based on the task of the suspended object, and an intelligent optimization algorithm is designed to plan an optimal desired trajectory for the suspended object to move stably and smoothly.

(3) Based on the kinematics and dynamics analysis of the suspension system, the tension space of the cable and the motion space of the suspended object are coincident. Considering the multi-robot cooperative constraints, an obstacle avoidance planning method is proposed using the consistency of force-position coordination.

(4) Based on the planned trajectories of the suspended object, the trajectories of the end of the towing robot are planned by the force-position cooperative optimization method, and the solution set of motion trajectory is obtained according to the cooperative relationship.

(5) Verification is conducted to ensure whether the planned trajectories meet the performance metrics. If not, the program ends and is re-planned. If so, the optimal trajectory for obstacle avoidance planning is recorded and saved.

3.2 Design of SDBO algorithm

The obstacle avoidance planning for the suspended object is to obtain a set of task points or trajectories that meet various constraints of the system and do not interfere between the towing robots, cables, and obstacles by using reasonable planning algorithms. Based on the start and end points of the towing, the intermediate target points are placed in the collision-free space to ensure that the suspended object is able to reach the end point while avoiding an obstacle. The trajectory planning that relies on heuristic algorithms is effective in determining these intermediate points and gradually brings them closer to the target point through iterative calculations. Compared to other heuristic algorithms, the DBO algorithm can adapt to different search stages and environments. The algorithm not only considers global ex-

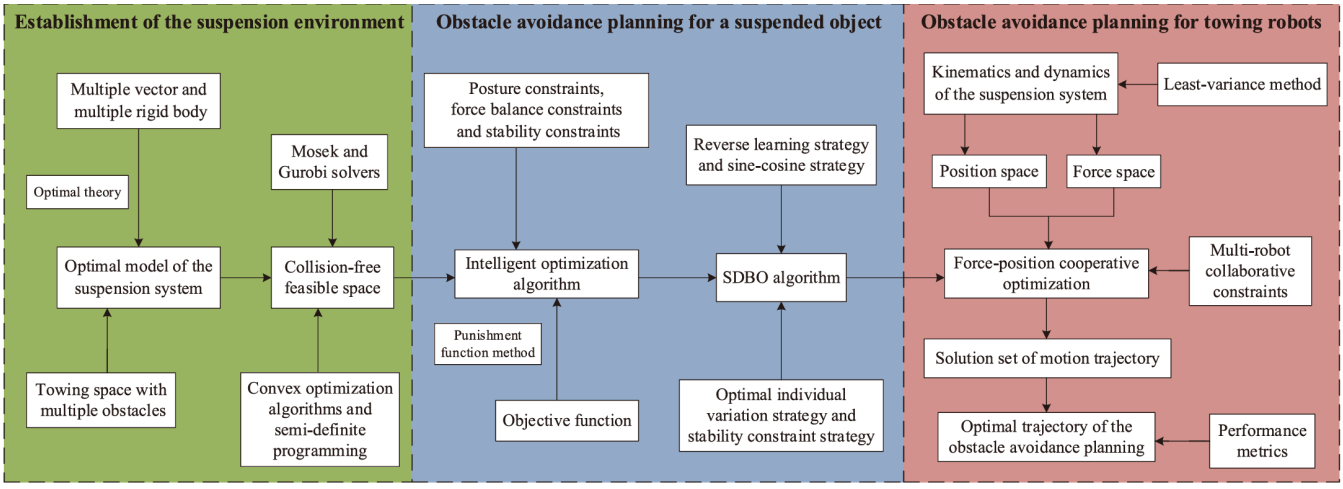

Figure 2 Obstacle avoidance planning for a multi-robot suspension system.

ploration to avoid falling into local optima, but also pays attention to local development to achieve fast convergence [32]. Considering the safety of trajectory planning for a suspension system, the stability constraint factor is introduced into the DBO, an advanced version, known as SDBO, is proposed to handle obstacle avoidance planning in a multi-robot suspension system.

Although the DBO algorithm has the characteristics of strong optimization ability and fast convergence speed, there are also disadvantages between global exploration and local development, which is easy to fall into local optimal and weak global exploration ability. To enhance the DBO search capabilities and the efficiency of trajectory planning, four improvements have been implemented in the DBO algorithm.

(1) The reverse learning strategy [38] is utilized to initialize the population, so that the distribution is more uniform, and the search ability is improved. The basic steps are as follows:

• The population (P) is randomly generated (the population size and dimension in order are denoted by N_P, and D).

• The reverse population OP is calculated.

$$OX_{ij} = a_j + b_j - X_{ij}, \tag{13}$$

where $i = 1, 2, \ldots, N_P$, $j = 1, 2, \ldots, D$, X_{ij} represents the j-th dimension value of the i-th individual in population P, OX_{ij} is the corresponding inverse solution, whereas a_j and b_j, respectively, is the minimum and maximum values of the j-th dimension in the search interval.

• The fitness function is used to select the individuals with high fitness from the set $\{P \cup OP\}$ as the initial population P_0.

(2) The sine-cosine strategy [39] is employed to establish a temporary population, update the location of individuals, increase population diversity, and avoid falling into local optimization.

The number of dung beetles was set to 30, and 20-30 were again divided, 20-25 still used the original method, whereas beetles 26-30 used the improved sine-cosine algorithm. First, the dynamic inertia weights are introduced to balance the local and global search capabilities, and then the parameter r_1 is changed from linear decreasing functions to exponential decreasing functions. The improved position update equation is as follows:

$$X_{ij}^{iter+1} = \begin{cases} w(iter) X_{ij}^{iter} + r_1 \cdot \sin(r_2) \cdot \left| r_3 P_j^{iter} - X_{ij}^{iter} \right|, & r_4 < 0.5, \\ w(iter) X_{ij}^{iter} + r_1 \cdot \cos(r_2) \cdot \left| r_3 P_j^{iter} - X_{ij}^{iter} \right|, & r_4 \geqslant 0.5, \end{cases} \tag{14}$$

where X_{ij}^{iter} denotes the position of the i-th dung beetle in the j-dimensional search space in the $iter$-th iteration; $r_2 \in [0, 2\pi]$, $r_3 \in [-2, 2]$, and $r_4 \in [-1, 1]$ represent the random numbers; P_j^{iter} signifies the position information of the optimal individual in the $iter$-th iteration; and finally, r_1 denotes an exponential decreasing function

$$r_1 = c \cdot \mathrm{e}^{-2\left(\frac{iter}{iter_{\max}}\right)^4}, \tag{15}$$

where c is a constant, $iter$ is the number of current iterations, and $iter_{\max}$ is the maximum number of iterations.

In addition, w represents the inertia weight in Eq. (9) per the following relation:

$$w(iter) = (w_{\max} - w_{\min}) - iter / iter_{\max}, \tag{16}$$

where $w_{\max}$ and $w_{\min}$ in order denote the maximum and minimum values of the inertial weights.

(3) The optimal individual variation strategy [40] is adoptedto mutate the global optimal solution, increase the diversity of the population, and enhance the ability to escape the local optimal. The improved equation for this strategy is given by

$$X_{ij}^{iter+1} = X_{ij}^{iter} + rand \cdot \left(X_{\text{best}}^{iter} - X_{ij}^{iter} \right), \tag{17}$$

where X_{best}^{iter} represents the global optimal solution, and $rand$ denotes a random number.

(4) The stability of the suspension system is mainly determined by the position of the suspended object and the minimum tension of the cable at the moment [41]. To more conveniently evaluate motion stability, these two factors are weighted by the position performance factor and the tension performance factor, respectively, and defined as the stability constraint factor (S_c) for the multi-robot coordinated suspension system.

$$S_c = \left(\mu_1 \lambda_p + \nu_1 \tau_p \right) \cdot \left(\mu_2 \lambda_q + \nu_2 \tau_q \right), \tag{18}$$

where λ_p and λ_q represent the position performance factors, τ_p and τ_q denote the tension performance factors, respectively, μ_1, μ_2, ν_1, and ν_2 are the weighting coefficients such that $\mu_1 + \mu_2 = 1$, and $\nu_1 + \nu_2 = 1$.

The stability constraint factor (S_c) is introduced into the DBO, and the position update equation at this time takes the following form:

$$X_{ij}^{iter+1} = S_c \cdot X_{ij}^{iter}, \tag{19}$$

where X_{ij}^{iter} denotes the position of the $iter$-th iteration. In general, $S_c \in [0, 1]$, and for the case of $S_c < 0.6$, the SDBO algorithm is able to constrain the position of the suspended object to update to the instability space. Additionally, in the case of $S_c > 0.6$, the suspended object is relatively stable, and the SDBO algorithm could maintain a certain searchability and convergence speed.

Obstacle avoidance planning with the SDBO algorithm

for a suspended object consists of several steps:

(1) The parameters of the suspension system were initialized, the information about the suspension environment was obtained, and the dung beetle population was initialized by Eq. (13).

(2) The position of dung beetles in the temporary population was updated by Eq. (14), a fitness function was selected, the fitness value was calculated, and the optimal position at current was obtained.

(3) The position of all dung beetles was updated by Eq. (17), and the fitness value of the updated position was calculated. Once a better fitness value is obtained, the optimal position of the current population is updated.

(4) The S_c was calculated by Eq. (18), if $S_c \in [0.6, 0.9]$, the updated position and fitness values were calculated by Eq. (19). If a better fitness value is obtained, the current optimal position and optimal fitness value will be updated, otherwise, the program will return to step (3) to recalculate.

(5) The above steps were repeated until the program reached the $iter = iter_{\max}$, and global optimal position and fitness value were exported.

(6) The optimal position that meets the conditions was added to the trajectory, and the globally optimal trajectory of the suspended object was obtained by using the Makima method for interpolation.

3.3 Collaborative optimization for force and position

The inverse solutions of multi-robot coordinated suspension system are fundamental for trajectory planning, which is not only a geometric problem but also a force problem. In a few cases, there are inverse solutions for the kinematics and dynamics of multi-robot coordinated suspension system, whereas in most cases, there are infinitely many solutions. Therefore, it is very important to optimize the inverse solution of the suspension system.

To enable the existence of inverse solutions for the suspension system, the inverse solution of the system is chosen according to the least-variance method, and the main reason for this is that the inverse solution obtained by the least-variance method is the one that is closest to the mean, and therefore the variation of the solution is relatively uniform and smooth [42]. The objective function can be defined as follows:

$$\psi = \min\left\{\sum_{\xi=0}^{\xi_{\max}}\left[\frac{1}{\eta-1}\left(\sum_{\vartheta=1}^{\eta}\Gamma_{\vartheta}^{\xi}-E^{\xi}(\Gamma)\right)^2\right]\right\}, \tag{20}$$

where Γ_{ϑ}^{ξ} is the solution of the optimized parameter ϑ at time ξ, η is the number of inverse solutions, and $E^{\xi}(\Gamma) = \left(\Gamma_1^{\xi}+\Gamma_2^{\xi}+\cdots+\Gamma_{\eta}^{\xi}\right)/\eta$ is the arithmetic average of the optimized parameter.

If Γ is the end position of the towing robot, the tension and the length of the cable, ψ represents the flatness of the end trajectory of the towing robot, the degree of the change of the tension, and the length of the cable.

During the towing process, it is necessary to give priority to ensuring the stability of the suspended object. Moving too fast may cause the instability of the suspended object or increase the risk of collision, so it is necessary to sacrifice some movement time in exchange for higher stability and safety. With the availability and safety of the system as the planning objective, the suspended object can avoid obstacles and the cable can achieve obstacle avoidance during the towing process according to the cooperative constraints of multiple towing robots. Taking the trajectory of the suspended object as the optimization variable, multiple performance metrics are integrated, the trajectory length of the suspended object f_1, the height of the suspended object f_2, the length of the cable f_3, the change rate of the cable tension f_4, and the curvature of the trajectory f_5 as the objective function, the penalty function f_6 is utilized to solve the optimal trajectory in the solution set of the motion trajectory. The fitness function can comprehensively evaluate the pros and cons of the solution by integrating multiple indexes, and avoiding the one-sidedness caused by a single index. To develop and test obstacle avoidance strategies, it is assumed that the weights of each index in the fitness function are equal. For this purpose, the fitness function is introduced, these are formulated as

$$f = f_1 + f_2 + f_3 + f_4 + f_5 + f_6, \tag{21}$$

where $f_1 = \sum_{d=1}^{n}\sqrt{(x_{d+1}-x_d)^2+(y_{d+1}-y_d)^2+(z_{d+1}-z_d)^2}$, (x_d, y_d, z_d) is the coordinate of the d-th discrete point, n is the total number of discrete points.

$f_2 = \sum_{d=1}^{n} z_d = \sum_{d=1}^{n}\left|z_d^{\text{end}} - z_d^{\text{start}}\right|$, z_d^{end} is the z coordinate of the d-th discrete point, z_d^{start} is the z coordinate at the reference plane.

$f_3 = \sum_{k=1}^{3} l_k$, $f_4 = \sum_{k=1}^{3} V_k = \sum_{k=1}^{3}\left(\frac{\partial \mathbf{T}_k}{\partial \imath}\cdot\frac{\partial\left(\mathbf{L}_k/\left\|\mathbf{L}_k\right\|\right)}{\partial \imath}\right)$, k represents the number of towing robots, $\imath$ is the movement time, $\mathbf{T}_k$ is the tension, l_k is the length of the cable.

$$f_5 = \sum_{d=1}^{n}\frac{1}{\rho} = \sum_{d=1}^{n}\frac{\Delta\chi}{L} = \sum_{d=1}^{n}\frac{\Delta\chi}{\sqrt{(x_{d+1}-x_d)^2+(y_{d+1}-y_d)^2+(z_{d+1}-z_d)^2}},$$

ρ is the curvature radius of the trajectory, L is the distance between adjacent two points, $\Delta\chi$ is the angle change between the line of adjacent two points and the tangent line of

the trajectory at that point.

$f_6 = \sum_{iter=1}^{iter_{\max}} \kappa n_p$, $iter$ represents the number of current iterations, $iter_{\max}$ represents the total number of iterations, $\kappa = 1000$ is set as the penalty factor, and n_p denotes the number of collisions between the trajectory and the obstacles at the current iteration.

In obstacle avoidance planning for multi-robot suspension system, constraints on the system need to be considered.

(1) Posture constraint: the posture angle $[\alpha_1, \alpha_2, \alpha_3]^{\mathrm{T}}$ of the suspended object should be less than a certain angle to ensure that there is no wrap and interference between the cables, and to reduce the phenomenon of virtual cable and unbalanced load distribution.

(2) Obstacle distance constraint: the distance $l(O_P, O_\gamma)$ between the suspended object, cables, robots, and obstacles is kept at a certain safe distance ϑ.

(3) Cable length constraint: the length of the cable must be within a certain range to ensure the stable towing of the suspended object.

(4) Cable tension constraint: the tension of the cable must be between the maximum allowable force T_{da} and the minimum preload force T_{xiao}, and the tension of the cable must be positive.

(5) Force balance constraint: the tension of the different cables should be close to that of them, and the tension coefficient $C_t = T_{\min} / T_{\max}$ is used to characterize. $T_{\max} = \max(T_1, T_2, T_3)$, $T_{\min} = \min(T_1, T_2, T_3)$. As the C_t approaches 1, the tension moves further away from the critical value, and as the C_t approaches 0, some of the tension moves closer to the critical value.

(6) Stability constraints: the stability S_c of the system must be large enough, and the movement of the suspended object must be controllable.

The constraint is defined as g_R, and its mathematical description is as follows:

$$\begin{cases} -10^\circ < [\alpha_1, \alpha_2, \alpha_3]^{\mathrm{T}} < 10^\circ, \\ l\left(O_P, O_\gamma\right) \geqslant \vartheta, \\ l_{\min} \leqslant l_k \leqslant l_{\max}, \\ 0 < T_{\mathrm{xiao}} \leqslant T_k \leqslant T_{\mathrm{da}} \leqslant T_{\mathrm{lim}}, \\ 0 < C_t \leqslant 1, \\ S_{c\min} \leqslant S_c, \end{cases} \tag{22}$$

where $l_{\min}$ and $l_{\max}$ are the minimum and maximum lengths of the cable, respectively. $T_{\mathrm{lim}} = k_a \cdot T_{\mathrm{da}}$ is the ultimate tension of the cable, $1.5 \leqslant k_a \leqslant 2$ is the safety factor. $S_{c\min}$ is the minimum stability of the system.

Considering the coincidence of the force space and position space, the obstacle avoidance planning is investigated based on the collaborative optimization for force and position. The optimal combination of trajectories is selected from multiple feasible motion trajectories to achieve the desired trajectory of the suspended object, while ensuring stable operation of the system and avoiding sudden changes of cable tension. In summary, the method of collaborative optimization for force and position is shown in Fig. 3.

The detailed steps are as follows:

(1) The towing environment of the suspension system was established, and the collision-free feasible space of the suspension system was calculated based on the known data of the static obstacle.

(2) Assuming that the ends of the three towing robots were located on the same horizontal plane, the position of the robots was determined based on the towing task, with the simultaneous assessment of keeping a safe distance by the robots. If the safe distance is not satisfied, adjustments are made to the position of the towing robot to ensure safety while detecting obstacles in the towing environment.

(3) The feasible trajectory of the suspended object was planned based on the SDBO algorithm. The desired trajectory of the suspended object was discretized by time interval Δt, the initial and end moments in order are represented by t_0 and t_f, and the tension and length of the cable were calculated from the constraints and the kinematic and dynamic model of the system. The feasible end position of the towing

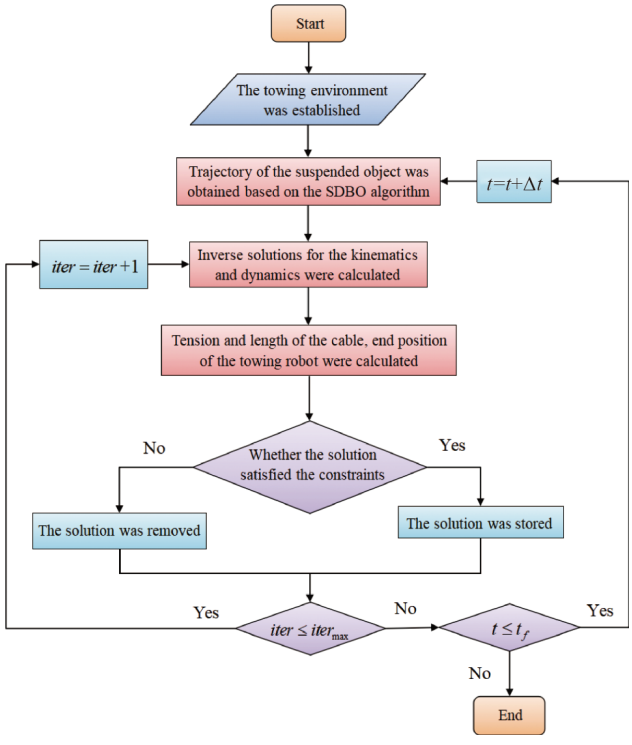

Figure 3 Collaborative optimization for force and position.

robot was selected according to the cooperative relationship.

(4) Verification is conducted to ensure whether the planned trajectories meet the constraint conditions was checked. When $iter \leqslant iter_{\max}$, the program was returned to step (3), otherwise, continued to perform step (5).

(5) Evaluation is performed to determine whether the multi-robot suspension system has reached the set target position or not. Making $t = t + \Delta t$, for the case of $t \leqslant t_f$, the program is returned to step (3), otherwise, the program is ended and the optimal or feasible trajectory of the multi-robot suspension system is exported.

4. Results and discussion

In a multi-robot suspension system, potential collisions involving towing robots, cables, suspended objects, and obstacles are analyzed through the proposed SDBO algorithm aimed at obstacle avoidance planning. The effectiveness of this approach is also verified through simulation using MATLAB R2023b. The test setup consisted of a Windows 10 system with an Intel Xeon-Gold 6226 processor and 512 GB memory, using the Mosek and Gurobi solvers to solve the collision-free feasible space in the suspension environment.

4.1 Establishment of the suspension environment

For aerial operations (maintenance of building exterior wall), downhole operations (oil and mine mining), and mountain rescue tasks, it is assumed that the multi-robot suspension system was driven in such a way that only the length of the cable was changed and the end positions of the robots were fixed. Multiple static obstacles are positioned in the towing area as per the towing task requirements. For this purpose, a suspended cylinder (The radius is 0.1 m, and a height is 0.3 m.) with a mass of 10 kg maintains a fixed posture to ensure safe towing. The cable's tension is allowed to vary between $T_{\min}$=1 N and $T_{\max}$ = 100 N. The position of the three towing robots in space is an equilateral triangle, and the structure of the robot is specified as follows: a_{k1} = 4 m, a_{k2} = 3 m, a_{k3} = 2 m, the position at the bottom of the robot are $O_1(0,5,0)$, $O_2(-2.5\sqrt{3},-2.5,0)$, and $O_3(2.5\sqrt{3},-2.5,0)$, respectively, and the robot's structure is sufficient to hold the robot at higher levels.

The suspended object can be considered as a particle in an ideal trajectory planning environment, and obstacle avoidance planning is the planning of the center of mass. However, the suspended object is a rigid body with mass and size in actual obstacle avoidance planning, so the shape and size of the suspended object should be considered to avoid collisions during the suspension process. A schematic diagram of the suspension environment is shown in Fig. 4, where the suspended object is represented by a red cylinder, the cable is represented by a cylinder, the end of the towing robot is represented by a sphere, whereas the other objects are obstacles. For irregular obstacles, these models can be optimized for typical examples using surround-box theory to obtain a more general model. The boundary of the obstacle and cable is expanded outward in the establishment of the suspension environment, and the warning area is established outside the obstacles. Once the suspended object and the cable enter the warning area, it will be considered a collision.

The environment information of the towing system is integrated to obtain the global environment information, and the intermediate target points are set along the motion path according to the requirements of the towing task. The global collision-free feasible space is obtained by calculating the collision-free space at each intermediate target point. Taking two-dimensional space as an example, the calculated collision-free feasible space is a convex polygon, as shown in Fig. 5, where the black polygon represents obstacles, the yellow straight line partitions the two-dimensional space into several convex polygons, the blue ellipse is the largest tangent ellipse in the convex polygon, and the pink curve is

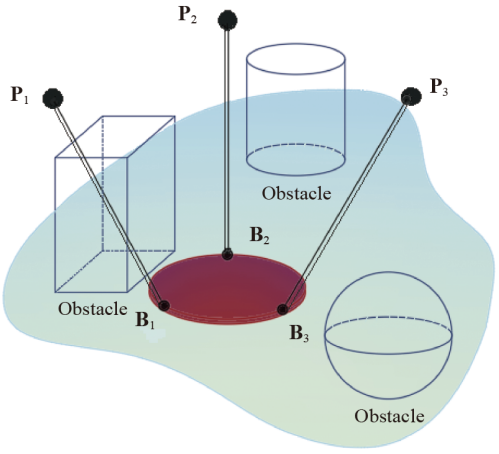

Figure 4 Schematic representation of the suspension environment.

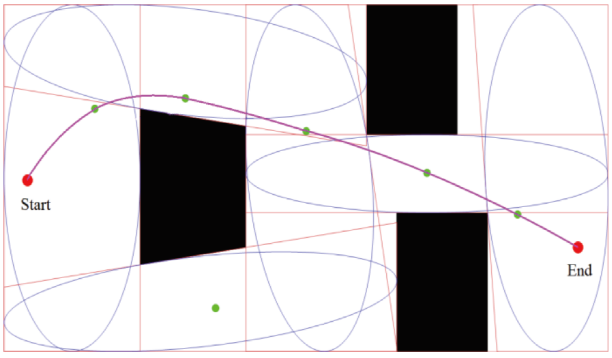

Figure 5 Collision-free feasible space in a two-dimensional spatial domain (note: the black units represent the obstacles, while the white ones denote the free space).

the obstacle avoidance trajectories planned in the collision-free feasible space. The red points are the starting and the ending points, whereas the green points are the intermediate target points.

Convex optimization algorithm and SDP are effective methods for solving the obstacle avoidance planning in multi-robot suspension systems [43]. The use of tangent ellipses in optimization algorithms can be considered as a strategy for finding optimal solutions in a confined space, especially when dealing with spatial optimization problems with obstacles in multi-robot suspension system. In environments with obstacles, the tangent ellipse can be used as the search boundaries to avoid obstacles. When the suspended object in the optimization algorithm updates its position, it can ensure that it does not exceed the scope of the tangent ellipse, thus avoiding entering the obstacle region. The convex optimization algorithm and SDP are used to solve the collision-free feasible region in the space, and the mathematical model is established as follows.

Our algorithm searches for both an ellipsoid and a set of hyperplanes which separate it from the obstacles. The tangent ellipsoid represents the largest circular region within a convex polyhedron and can be seen as an approximation or starting point for finding an optimal solution within that region. We choose to represent the ellipsoid as an image of the unit ball: $\varepsilon(\mathbf{C},\boldsymbol{\beta}) = \{\phi = \mathbf{C}\tilde{\phi} + \boldsymbol{\beta} \mid \| \tilde{\phi} \| \leqslant 1\}$. We have chosen this definition of the ellipsoid because it makes maximization of the ellipsoid volume straightforward: the volume of the ellipsoid is proportional to the logarithm of the determinant of $\mathbf{C}$, which is a concave function of $\mathbf{C}$ and can therefore be efficiently maximized. The problem of finding the maximum volume ellipsoid contained in a polyhedron $M = \{\phi \mid \mathbf{A}\phi \leqslant \boldsymbol{\delta}\}$ can be expressed as

$$\begin{aligned} &\underset{\mathbf{C},\boldsymbol{\beta}}{\text{maximize}} \ \log\det\mathbf{C}, \\ &\text{subject to} \ \left\| \mathbf{q}_\gamma^{\mathrm{T}}\mathbf{C} \right\| + \mathbf{q}_\gamma^{\mathrm{T}} \leqslant \delta_\gamma, \\ &\gamma = 1, 2, \ \ldots, \ N_{ob}, \ \ \mathbf{C} \geqslant 0, \end{aligned} \tag{23}$$

where $\mathbf{q}_\gamma$ is a row of $\mathbf{A}$, δ_γ is the element of $\boldsymbol{\delta}$, and γ is the number of obstacles.

The flow of the algorithm and the specific steps are shown in Fig. 6.

Therefore, the critical support lines between the obstacles are taken as constraints, the collision-free feasible space of the system is obtained by using convex optimization algorithms and SDP in the suspension environment, and then obstacle avoidance planning is performed in this space to ensure the stability of the towing process.

4.2 Simulation and analysis

4.2.1 Implementation and results of the SDBO algorithm

To verify the ability of the SDBO algorithm in the presence of various suspension environments and different towing tasks, obstacle avoidance planning simulation experiments were conducted on different numbers of obstacles as well as different starting points and end points. In addition to employing the SDBO algorithm for obstacle avoidance planning for suspended objects, other optimization algorithms, namely DBO [31], PSO [44], and GA [45] were selected for comparative analysis to mitigate errors. All algorithms share the same parameters, the number of iterations is $iter_{\max} = 500$, and each algorithm is independently run 20 times.

The planning results of the four algorithms are demonstrated in Fig. 7, where the curves in green, red, blue, and black represent the trajectories with the same start and end points but different trajectories. The left graph shows a 3D view of the optimal trajectory of the suspended object, and the right graph displays the top view. The performance metrics obtained from the simulations are presented in Table 1. The proposed SDBO algorithm is evaluated for validity by comparing key metrics such as the minimum (Min), maximum (Max), average value (Average), standard deviation (Std) of the fitness function, length, height, and runtime (Rt) of the planned trajectory of the suspended object, and

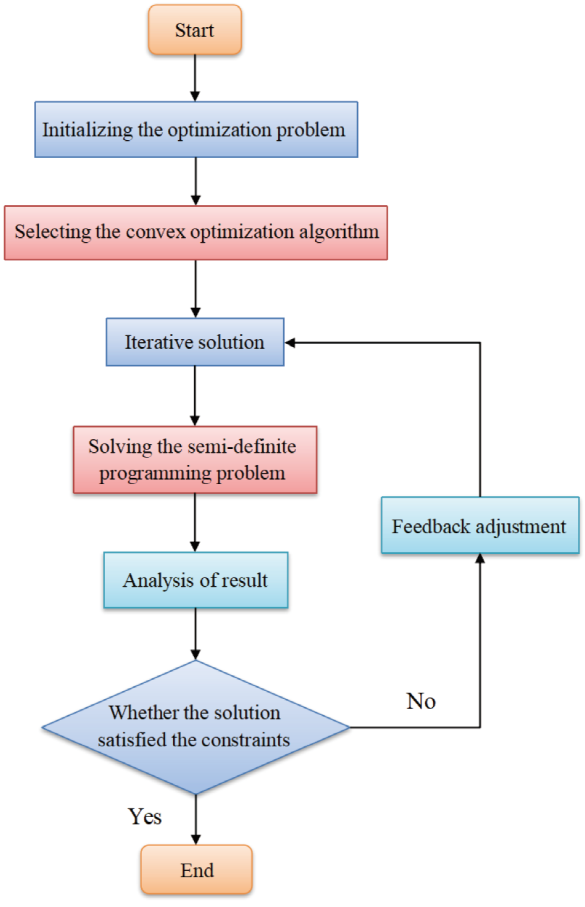

Figure 6 Algorithm flow.

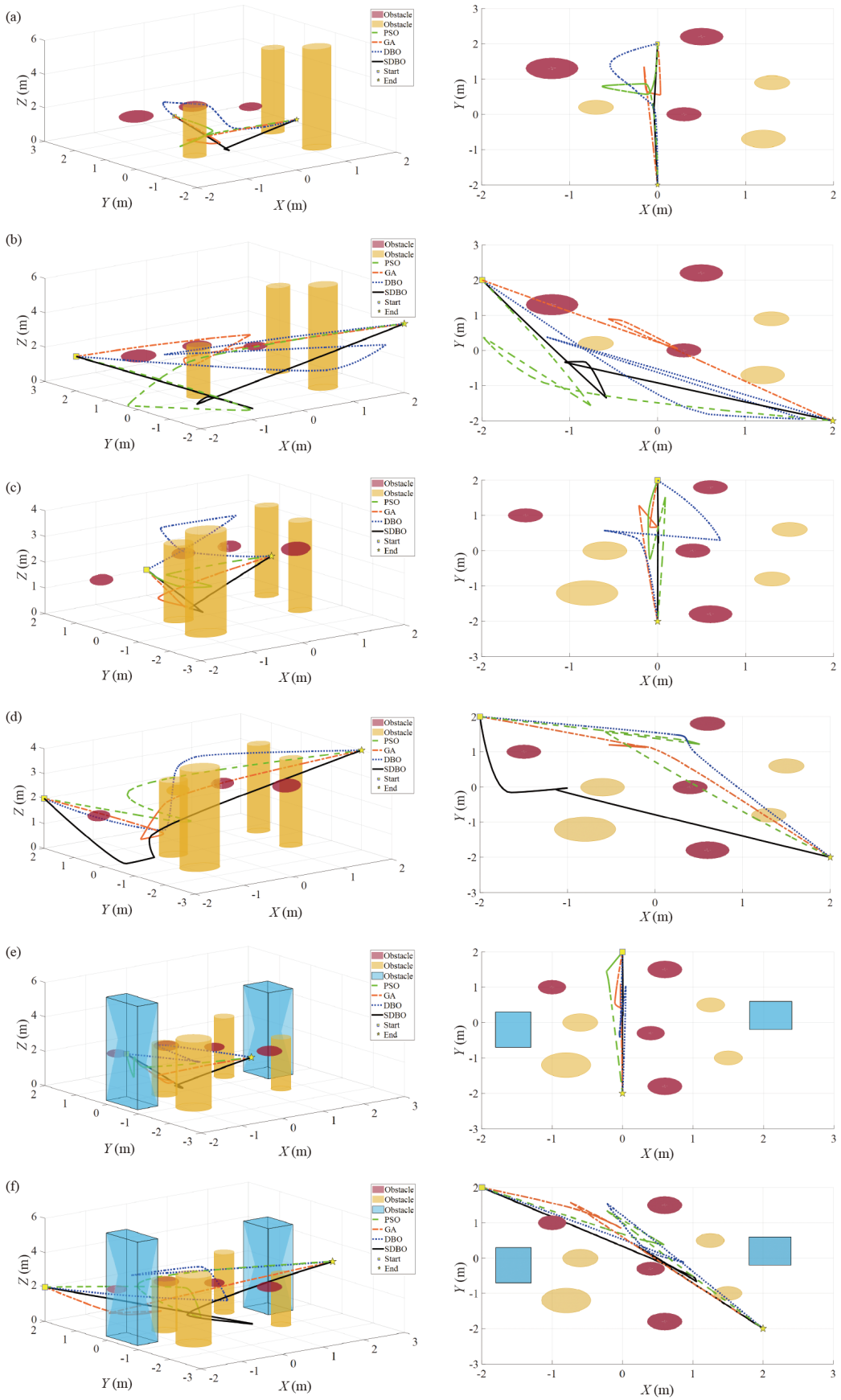

Figure 7 Spatial trajectories of the suspended object and projection in the *XOY* plane: (a)-(f) scenarios 1-6.

Table 1 Optimization results based on different algorithms

Scenario	Obstacles	Start and end points	Algorithm	Fitness function				Suspended object			
				Min	Max	Average	Std	Length (m)	Height (m)	Curvature radius (m)	Rt (s)
1	6	(0, 2, 1) (0, −2, 3)	PSO	163.2861	725.9113	373.4791	195.6208	6.8343	33.8985	94.4987	28.09
			GA	82.5887	666.2122	299.2193	213.1286	6.5145	20.2559	75.1116	21.21
			DBO	1635.7029	9251.2176	4201.1047	1904.3170	7.0727	83.0597	28.0580	47.62
			SDBO	68.0011	540.9792	219.9053	159.7733	6.0464	16.7108	165.2960	18.17
2	6	(−2, 2, 2) (2, −2, 4)	PSO	468.9918	3366.4605	1055.8537	823.0569	13.6374	47.5234	48.8077	35.97
			GA	143.4318	2920.7602	749.3265	607.0223	10.8760	69.0041	43.1651	27.26
			DBO	2134.6594	18327.0849	11753.4337	4359.5154	14.1879	77.5109	30.7199	52.30
			SDBO	111.9462	791.6384	487.3101	193.5753	10.3791	22.1613	50.9103	24.92
3	8	(0, 2, 1) (0, −2, 3)	PSO	121.4941	2890.8713	798.7120	972.2448	8.2004	47.7682	68.7023	25.23
			GA	80.4262	4926.2746	698.5098	1213.9177	6.7221	20.8926	54.4214	20.95
			DBO	196.9785	11005.3337	3640.5283	2864.6942	8.0079	113.1798	30.5793	29.93
			SDBO	68.2625	4821.4101	1124.6991	1475.6832	6.4443	16.8559	73.0342	18.44
4	8	(−2, 2, 2) (2, −2, 4)	PSO	139.0732	922.1477	579.5371	276.3410	9.8696	55.9211	63.9336	26.64
			GA	128.9965	935.2643	553.0758	300.0983	9.1488	44.4128	87.4662	26.08
			DBO	4211.9914	14661.5823	9534.8651	3694.5592	9.5764	83.9083	93.3612	61.63
			SDBO	126.6233	890.3857	514.8325	274.1910	9.3092	35.7651	99.3391	25.71
5	10	(0, 2, 1) (0, −2, 3)	PSO	111.0002	3050.5225	1004.6129	1102.4425	6.8603	36.4788	128.2953	24.25
			GA	78.9122	1861.9012	655.5810	702.9734	6.7282	22.9033	32.2278	20.23
			DBO	584.1079	11608.2546	5534.2821	3071.4407	7.2782	77.1199	25.6392	38.12
			SDBO	68.3896	1742.5989	445.9664	799.8293	6.1458	16.9658	80.8673	18.63
6	10	(−2, 2, 2) (2, −2, 4)	PSO	141.1316	1051.4608	638.5441	343.2190	11.4768	64.5769	49.2749	26.85
			GA	111.8865	1134.1511	608.5200	316.3575	10.1865	32.5523	80.5726	24.83
			DBO	4705.4743	18770.2169	9854.5740	4046.9197	12.1903	91.6598	48.3046	68.30
			SDBO	111.6006	921.2907	479.7162	267.4654	10.5816	30.0777	83.1536	24.65

the curvature radius is taken as a rational measure to describe the smoothness of the trajectory.

All algorithms are capable of effectively finding a safe trajectory, as depicted in Fig. 7, the trajectories generated by the SDBO algorithms are characterized by smoother profiles with fewer abrupt changes. In cases where the height of the obstacle is minimal, the suspended object passes over the obstacle. On the contrary, when a taller obstacle is encountered, the suspended object circumvents it from the side to ensure system stability, aligning more closely with practical obstacle avoidance strategies.

Although the four algorithms were able to obtain the optimal value as presented in Table 1, the SDBO algorithm demonstrated superior performance in almost all metrics, exhibiting enhanced stability and optimization coordination in comparison to the other three algorithms. For example, considering scenario 1, the SDBO algorithm outperforms the DBO algorithm and reduces the length of the suspended object by 14.51% and the height by 79.88%. The results show that the SDBO algorithm can solve the shortest trajectory more efficiently and quickly, and it avoids the problem that PSO, GA, and DBO can easily fall into the local optimization.

4.2.2 Simulation results for obstacle avoidance planning

The acceleration of the suspended object has a direct effect on the cable tension and subsequently affects the end position of the towing robot. Hence, gentle and smooth acceleration during the towing operation contributes to the overall stability of the towing robot. For example, considering scenario 1, Fig. 8 illustrates the time-history plots of the position, velocity, acceleration, and jerk of the suspended object along the X, Y, and Z axes, respectively.

As can be seen from Eqs. (4)-(6), the acceleration of the suspended object directly affected the cable tension, which in turn affected the end position of the towing robot. The time history of the acceleration of the suspension is gentle and smooth, which is conducive to the stability of the towing robot. The trajectories in Fig. 8 are stable, the trajectories planned by the SDBO algorithm are characterized by smoother profiles with fewer abrupt changes, the SDBO algorithm is able to present the suspended object with lower acceleration in almost all directions compared to other approaches. Analysis of the acceleration revealed that SDBO exhibited the highest optimization capability, followed by PSO and GA, with DBO displaying the least performance.

To ensure precise adherence to the planned trajectory by the towing robot, the trajectory of the suspended object is discretized into 40 path points, so that the trajectory of each cable can be one-to-one corresponding to these discrete points. The obstacle avoidance planning at each point ensures that the entire cable path does not collide with the

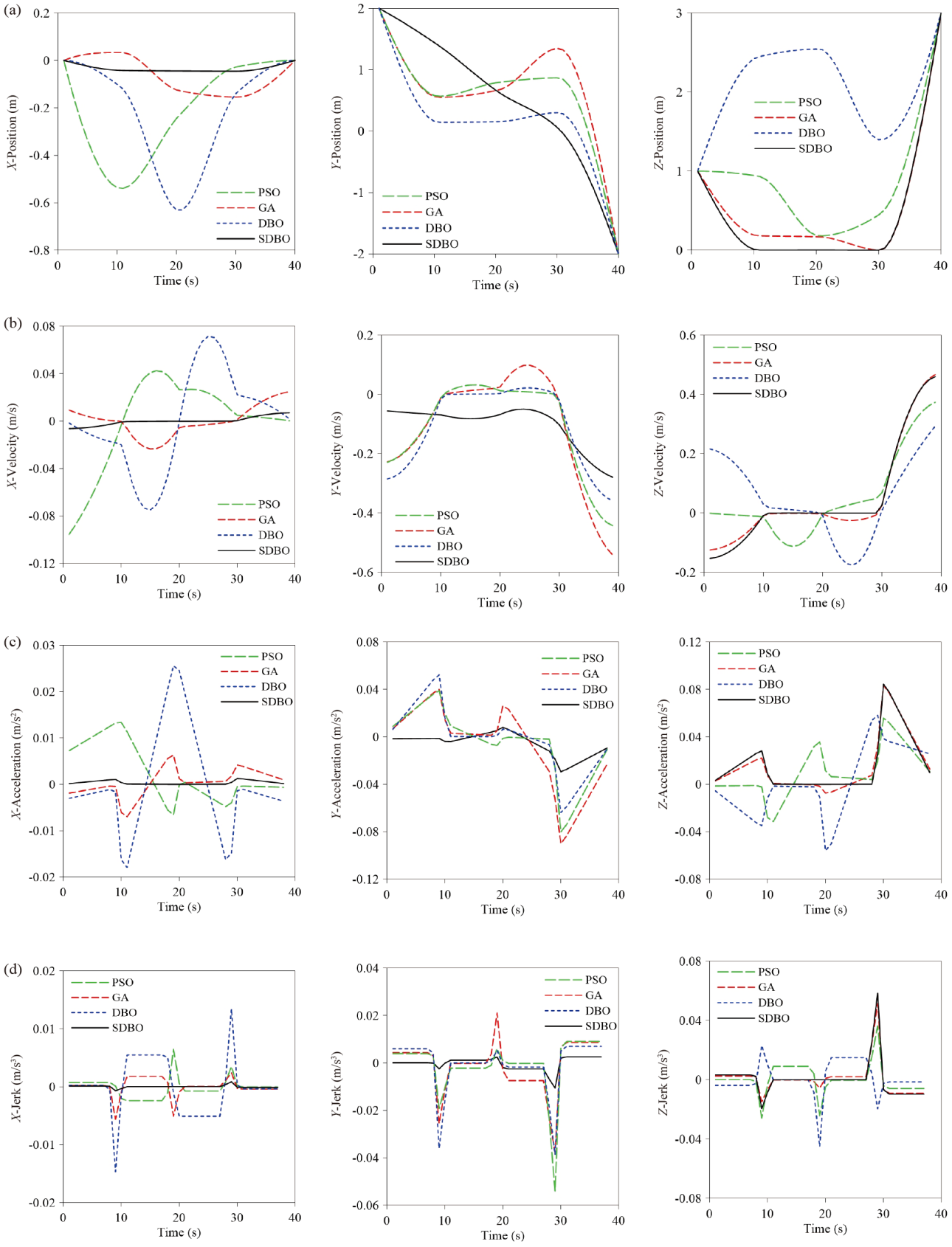

Figure 8 Three-dimensional kinetic properties of the trajectories of the suspended object based on various approaches: (a) position; (b) velocity; (c) acceleration; (d) jerk.

obstacle. The SDBO algorithm is employed to plan trajectories, with obstacle avoidance planning results for the suspension system depicted in Fig. 9. The midpoints of the suspended object are represented by a sequence of black cylinders, while the trajectories of the three cables are illustrated by thin solid lines in yellow, blue, and pink. The length and tension of the cable are further detailed in Fig. 10.

Figure 9 illustrates the collaborative operation of the three towing robots in towing an object to its desired position in the presence of obstacles in a multi-robot suspension system. When the cable encounters an obstacle, it can avoid the obstacle by adjusting the length of the cable. In the case of multiple solutions to the inverse kinematics of the suspension system, to ensure a continuous change in the length of the cable, the cable is rotated at a small angle each time to explore multiple feasible positions. By evaluating the safety of each position, an optimal solution can be selected to achieve cable obstacle avoidance. It can be seen from Fig. 10 that the changing trend of the cable length and cable tension is reasonable, and the cable is well able to avoid obstacles, which verifies the rationality of the trajectory of the suspended object.

It can be seen from Figs. 8-10 that when the suspended object moves along the trajectory planned by the SDBO algorithm, due to the symmetry of the spatial position of the towing robots 2 and 3, the length of cables 2 and 3 changes similarly and increases gradually while the length of cable 1 decreases. Since the towing robot 1 is the furthest from the suspended object at the initial time (0 s), the minimum tension of cable 1 is 1.5928 N. When the suspended object moves along the planned trajectory to approach the target position, cable 1 reaches the maximum tension of 96.5688 N at 40 s, while the tension of cables 2 and 3 begins to decrease, and the minimum tension at 40 s is 5.1757 and 7.9184 N, respectively. The tension of the cables is continuous and stable and is within the permissible tension range $1 \leqslant \mathbf{T}_k \leqslant 100$ N in Fig. 10, and there is no virtual pull phenomenon (the tension of the cable is less than 0), which verifies the rationality of the obstacle avoidance planning.

4.3 Comparison and analysis

Minimum fitness focuses on improvement in the worst individuals, while average fitness focuses on average performance across the population. Together, these two metrics

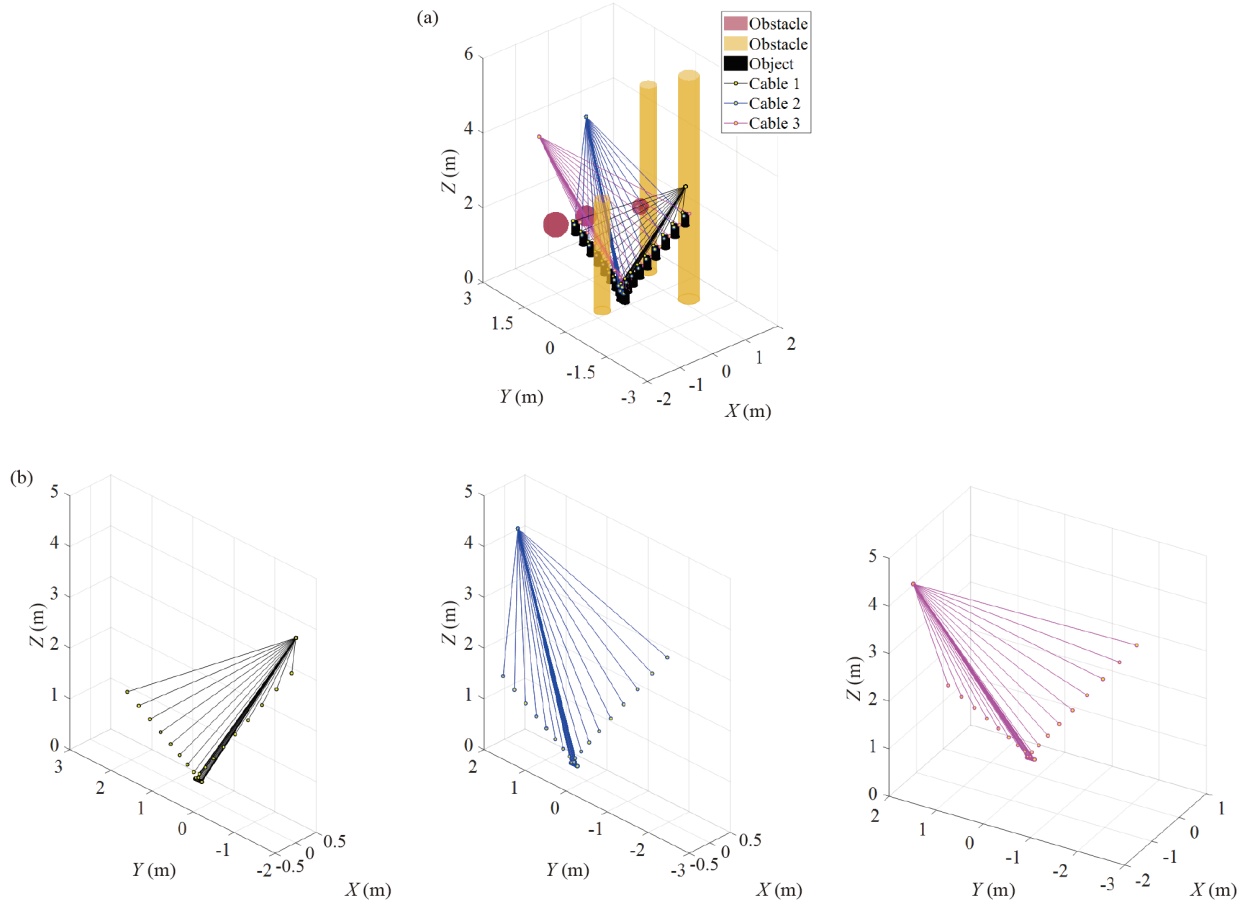

Figure 9 Spatial trajectories of the suspension system in the SDBO algorithm: (a) results for the obstacle avoidance planning; (b) trajectory of the cables.

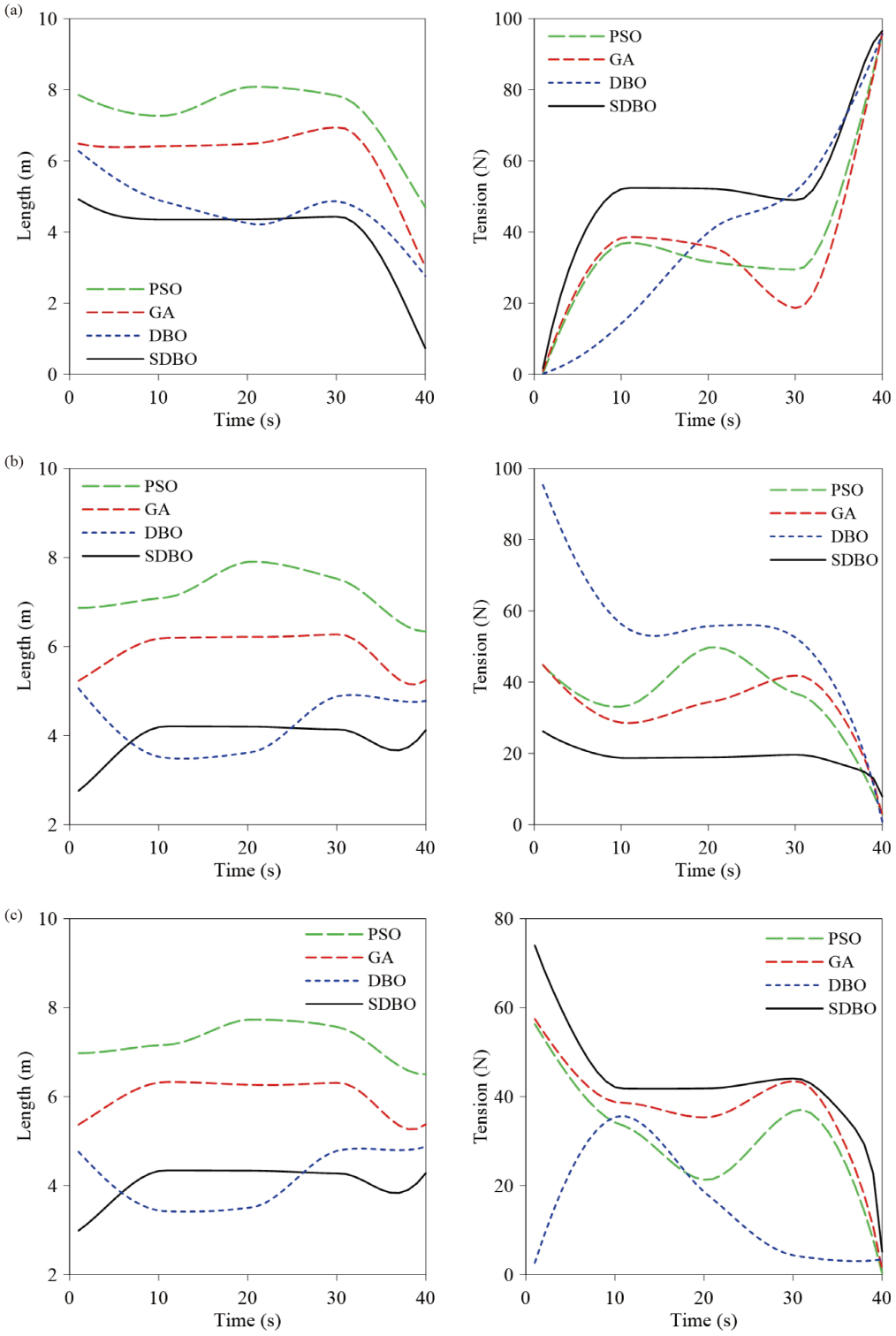

Figure 10 Length and tension of the cables: (a)-(c) cables 1-3.

can help researchers evaluate the performance of the SDBO algorithm and the evolutionary status of the population. For example, considering scenario 1, the convergence curve of the average fitness over 500 iterations has been demonstrated in Fig. 11 (the vertical axis is a logarithmic value), and the minimum fitness of 20 runs is presented in Fig. 12.

As can be seen in Fig. 11, the curves of SDBO, PSO, and GA show rapid convergence in the early stages of optimization, tending to plateau as the number of iterations increases. In particular, the SDBO algorithm demonstrates a

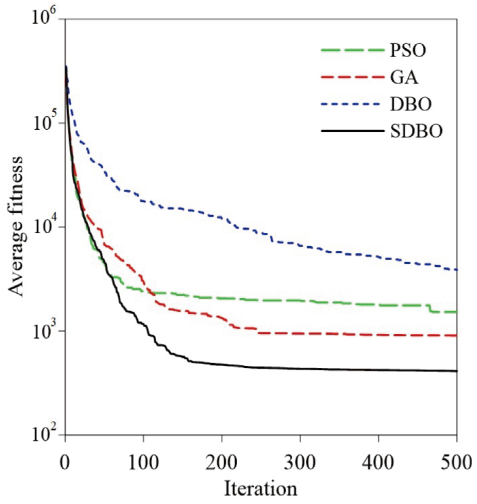

Figure 11 Convergence curves of various algorithms.

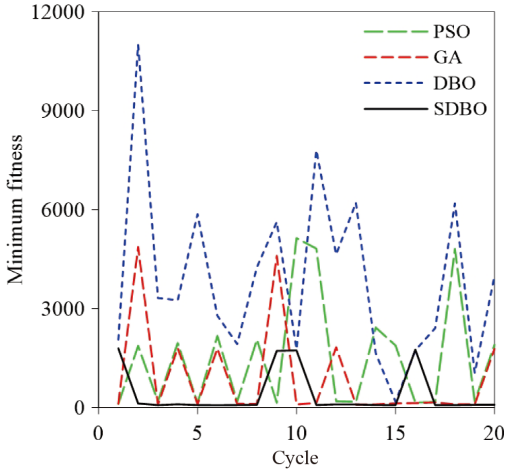

Figure 12 Minimum fitness of various algorithms.

rapid decrease across the iterations, leading to the achievement of the shortest trajectory length of about 150 iterations. Conversely, the DBO algorithm converges slowly and the resulting trajectory did not reach the optimum value. Compared with other algorithms, the SDBO algorithm exhibits superior optimization performance in terms of convergence speed and stability, and the GA algorithm closely follows it. The SDBO algorithm achieves the best results compared with various algorithms from Fig. 12, while the DBO and PSO algorithms can not find the optimal value. As can be seen in Figs. 11 and 12, the SDBO algorithm outperforms the DBO algorithm through reducing the minimum fitness by 95.84% and the average fitness by 94.77%. It is confirmed that the SDBO algorithm has superior optimization capability in complex environments with obstacles, and the improved strategy for the DBO algorithm achieves the desired effect.

The planning of the end position of the towing robot is an important guarantee of achieving the desired trajectory of the suspended object. The end position of the towing robot is fixed in the suspension system, and the end position of the towing robot determines the changing trend of the length and tension of the cable, so the initial position of the end of the towing robot needs to be optimized. The optimal position of the end of the towing robot obtained by the four optimization algorithms is shown in Table 2, and the maximum of the cable length is shown in Table 3.

According to the kinematics and dynamics of the suspension system, the end position of the towing robot affects the position of the suspended object, which in turn affects the length and tension of the cable. Therefore, the appropriate end position of the towing robot is conducive to the stable operation of the multi-robot suspension system. It can be seen from Table 2 that the height of the towing robot's end obtained by the SDBO algorithm is the lowest, which is beneficial for the stable operation of the system. It can be seen from Table 3 that the optimal length of the cable (the sum of the lengths of the three cables) is 19.5424, 16.2143, 23.7256, and 13.4705 m, respectively, the length of the cable corresponding to the optimal end position of the towing robot obtained by the SDBO algorithm achieve the best results.

Since the coincidence between the position space of the suspended object and the tension space of the cable, there are multiple solutions for the inverse kinematics and inverse dynamics of the suspension system, which creates challenges in solving the motion planning of the system. In this paper, obstacle avoidance planning is performed based on a collaborative optimization method for force and position, the results show that the suspended object moves smoothly, the length and tension of the cable are continuous and stable, and there is no mutated phenomenon, which verified it is feasible to solve simultaneously the tension and length of the cable using this optimization method. Unlike Ref. [26], which only deals with two-dimensional planar obstacle avoidance planning, the planning approach presented here is deemed more practical and enhances the safety and efficiency of suspension operations.

Table 2 Optimal position of the end of the towing robot based on various algorithms

Algorithms	Robot 1 (m)	Robot 2 (m)	Robot 3 (m)
PSO	(0.0191, −1.9903, 6.3300)	(1.3419, 1.9812, 6.3300)	(−1.7923, 1.9751, 6.3300)
GA	(0.0342, −1.9937, 6.0618)	(−1.7314, 1.4819, 6.0618)	(0.1299, 1.9670, 6.0618)
DBO	(0.0383, −2, 8)	(1.4306, 1.9208, 8)	(−1.8526, 2, 8)
SDBO	(0.0133, −1.9955, 4.0293)	(0.3110, 1.9869, 4.0293)	(−1.1305, 1.9884, 4.0293)

Table 3 Maximum of the cable length based on various algorithms

Algorithms	Cable 1 (m)	Cable 2 (m)	Cable 3 (m)
PSO	6.9437	6.2712	6.3275
GA	6.2797	5.0596	4.8750
DBO	8.0860	7.9064	7.7332
SDBO	4.9216	4.2047	4.3442

4.4 Discussion

The trajectories of the suspended object, length, and tension of the cable are presented in Figs. 8-10. Since the robots are considered as rigid bodies, these results are not sufficiently accurate, especially those related to the z-direction. As a general rule, considering the flexural flexibility of the robots, it is expected that the period's time of vertical displacement of the suspended object will be increased, length and tension of the cable will change more sophisticated.

In obstacle avoidance planning for multi-robot suspension system, the inertial term may not have a significant effect on the obstacle avoidance planning if the movement velocity of the suspended object is relatively low. When the movement velocity of the suspended object is high, the inertial force directly affects the acceleration of the suspended object and thus its trajectory. If the inertial term is neglected, it may lead to inaccurate obstacle avoidance paths and increase the risk of collision. The movement velocity of the suspended object studied in this paper is relatively low, so the inertial term may not be the main influencing factor, and it can be temporarily neglected when solving the system dynamics equations, especially in the initial stages of obstacle avoidance planning.

The DBO algorithm is improved by using existing techniques in this paper, and the obstacle avoidance planning method based on force-position coordination is used to solve the obstacle avoidance problem for multi-robot suspension system. However, according to the simulation results of this paper and the existing research results [46,47], the obstacle avoidance method still has some shortcomings: (1) as can be seen from the running time of Table 1, the obstacle avoidance planning method requires a lot of calculation, which may reduce the real-time performance of the algorithm; (2) in specific application scenarios, the obstacle avoidance planning method may perform well, but its universality and adaptability may be limited, especially in the changeable and unpredictable actual working environment, and algorithm improvement are needed to achieve better obstacle avoidance planning results.

Based on Refs. [19,36], it can be seen that multi-robot coordinated suspension system is a new type of towing equipment with great potential in practical application, subsequent work will focus on two aspects: (1) to make the stable operation of the suspension system, the weight of each optimization object is considered, and the multi-objective optimization algorithm suitable for multiple evaluation indexes is studied; (2) considering that there are many dynamic obstacles and constantly changing tasks in reality, dynamic obstacle avoidance planning of the suspension system is conducted.

5. Conclusions

The multi-robot suspension system consists of a closed loop of multiple towing robots, cables, and a suspended object. The force space of the cable and position space of the suspended object coincide, and the consisting elements affect each other. The previous research works only made the obstacle avoidance of the suspended object in the workspace and did not consider the obstacle avoidance of the cable and the towing robot. To fill this scientific gap, this paper takes into account the availability and safety of the multi-robot suspension system as the main planning objective, considers the coincidence of the force space and motion space, and presents a step-by-step optimization approach for force-position coordination to achieve three-dimensional obstacle avoidance planning for the system. The obtained results indicated that the SDBO algorithm demonstrated superior performance in all metrics, showing stability and optimization coordination in comparison to the other three algorithms. The suspended object and the cable are well able to avoid obstacles, and the changing trend of the cable length is reasonable, the tension of the cables is continuous and stable. The results provide a fairly solid theoretical basis for safe and stable towing tasks, as well as an appropriate basis for control implementation and generalization of the system.

Conflict of interest *On behalf of all authors, the corresponding author states that there is no conflict of interest.*

Author contributions *Xiangtang Zhao designed the study, established the models, and wrote the manuscript. Zhigang Zhao contributed to the simulation experiments, the result interpretation, and the manuscript revision. Cheng Su contributed to the design and discussion of the study. Jiadong Meng contributed to the data analysis and manuscript revision. Hutang Sang modified the language related issues. All authors revised the manuscript and approved the submission.*

Acknowledgements *This work was supported by the Excellent Graduate Student "Innovation Star" project of Education Department of Gansu Province (Grant No. 2025CXZX-675), the National Natural Science Foundation of China (Grant No. 51965032), the National Natural Science Foundation of Gansu Province of China (Grant No. 22JR5RA319), the Excellent Doctoral Student Foundation of Gansu Province of China (Grant No. 23JRRA842), the Open Project of State Key Laboratory of Rail Transit Vehicle System, Southwest Jiaotong University (Grant No. RVL2411), and the Key Research and Development Project of Lanzhou Jiaotong University (Grant No. LZJTU-ZDYF2302).*

1 H. Jamshidifar, A. Khajepour, and A. H. Korayem, Wrench feasibility and workspace expansion of planar cable-driven parallel robots by a novel passive counterbalancing mechanism, IEEE Trans. Robot. **37**, 935 (2021).

2 Z. Zhang, H. H. Cheng, and D. Lau, Efficient wrench-closure and

interference-free conditions verification for cable-driven parallel robot trajectories using a ray-based method, IEEE Robot. Autom. Lett. **5**, 8 (2020).
3 B. Zhang, W. Shang, S. Cong, and Z. Li, Coordinated dynamic control in the task space for redundantly actuated cable-driven parallel robots, IEEE ASME Trans. Mechatron. **26**, 2396 (2021).
4 I. Ben Hamida, M. A. Laribi, A. Mlika, L. Romdhane, S. Zeghloul, and G. Carbone, Multi-Objective optimal design of a cable driven parallel robot for rehabilitation tasks, Mech. Mach. Theory **156**, 104141 (2021).
5 J. He, G. Wen, and J. Liu, A class of bionic hyper-redundant robots mimicking the bird's neck, Acta Mech. Sin. **39**, 522351 (2023).
6 C. Passarini, D. Zanotto, and G. Boschetti, Dynamic trajectory planning for failure recovery in cable-suspended camera systems, J. Mech. Robotics **11**, 021001 (2019).
7 K. Mohammadi, S. Sirouspour, and A. Grivani, Passivity-based control of multiple quadrotors carrying a cable-suspended payload, IEEE ASME Trans. Mechatron. **27**, 2390 (2022).
8 K. Mohammadi, S. Sirouspour, and A. Grivani, Control of multiple quad-copters with a cable-suspended payload subject to disturbances, IEEE ASME Trans. Mechatron. **25**, 1709 (2020).
9 K. Mohammadi, M. Jafarinasab, and S. Sirouspour, in Decentralized motion control in a cabled-based multi-drone load transport system: Proceedings of the 2018 IEEE/RSJ International Conference on Intelligent Robots and Systems (IROS), Spain, 2018.
10 I. Maza, K. Kondak, M. Bernard, and A. Ollero, Multi-UAV cooperation and control for load transportation and deployment, J. Intell. Robot. Syst. **57**, 417 (2010).
11 K. Kondak, M. Bernard, F. Caballero, I. Maza, and A. Ollero, Cooperative autonomous helicopters for load transportation and environment perception, Adv. Robot. Res. 299 (2009), doi: 10.1007/978-3-642-01213-6_27.
12 N. Michael, J. Fink, and V. Kumar, Cooperative manipulation and transportation with aerial robots, Auton. Robot. **30**, 73 (2011).
13 Q. Jiang, and V. Kumar, The inverse kinematics of cooperative transport with multiple aerial robots, IEEE Trans. Robot. **29**, 136 (2013).
14 S. Xiang, H. Gao, Z. Liu, and C. Gosselin, in Trajectory optimization for a Six-DOF cable-suspended parallel robot with dynamic motions beyond the static workspace: Proceedings of 2020 IEEE International Conference on Robotics and Automation (ICRA), Paris, 2020, pp. 3903-3908.
15 S. Kamada, T. Laliberte, and C. Gosselin, in Kinematic analysis of a 4-DOF parallel mechanism with large translational and orientational workspace: Proceedings of 2019 International Conference on Robotics and Automation (ICRA) Montreal, 2019, pp. 1637-1643.
16 A. F. Cote, P. Cardou, and C. Gosselin, in A tension distribution algorithm for cable-driven parallel robots operating beyond their wrench-feasible workspace: Proceedings of the 16th International Conference on Control, Automation and Systems (ICCAS), Gyeongju, 2016.
17 M. Yamamoto, N. Yanai, and A. Mohri, Trajectory control of incompletely restrained parallel-wire-suspended mechanism based on inverse dynamics, IEEE Trans. Robot. **20**, 840 (2004).
18 C. Su, J. N. Ye, and W. Li, Analysis of dynamic workspace for under-constrained coordinate suspending system with multi-robots (in Chinese), J. Shanghai Jiaotong Univ. **53**, 225 (2019).
19 C. Su, X. Zhao, Z. Yan, Z. Zhao, and J. Meng, Workspace analysis of a floating multi-robot coordinated lifting system, J. Mar. Sci. Appl. **23**, 148 (2024).
20 H. Zhu, F. M. Claramunt, B. Brito, and J. Alonso-Mora, Learning interaction-aware trajectory predictions for decentralized multi-robot motion planning in dynamic environments, IEEE Robot. Autom. Lett. **6**, 2256 (2021).
21 T. Zhao, B. Zi, S. Qian, and J. Zhao, Algebraic method-based point-to-point trajectory planning of an under-constrained cable-suspended parallel robot with variable angle and height cable mast (in Chinese), Chin. J. Mech. Eng. **6**, 33 (2018).
22 J. Lin, B. Zi, and X. Wu, Research of cooperation obstacle avoidance planning for hoisting multi-robot system (in Chinese), Autom. Instrum. **27**, 5 (2012).
23 Z. K. Li, Y. Q. Huang, and Y. Q. Xu, Improved variable-step ant colony algorithm for mobile robot path planning, J. Electron. Meas. Instrum. **34**, 15 (2020).
24 B. K. Patle, D. R. K. Parhi, A. Jagadeesh, and S. K. Kashyap, Matrix-Binary Codes based Genetic Algorithm for path planning of mobile robot, Comput. Electrical Eng. **67**, 708 (2018).
25 Y. Ma, M. Hu, and X. Yan, Multi-objective path planning for unmanned surface vehicle with currents effects, ISA Trans. **75**, 137 (2018).
26 S. Qian, P. F. Qian, and C. H. Wang, Dynamics and path planning of multi-crane cooperative lifting robot, J. Mech. Eng. **58**, 20 (2022).
27 U. A. Mishra, I. Chawla, and P. M. Pathak, in On determining shortest path in joint space of a cable-driven parallel robot for point-to-point motion: Proceedings of the 28th Mediterranean Conference on Control and Automation (MED), Saint-Raphaël, 2020, pp. 984-989.
28 Z. Zhen, D. Xing, and C. Gao, Cooperative search-attack mission planning for multi-UAV based on intelligent self-organized algorithm, Aerospace Sci. Tech. **76**, 402 (2018).
29 Y. Li, X. R. Xu, and H. Xu, Three-dimensional trajectory planning of aerial robot based on ant colony algorithm, J. Anhui Univ. Tech. **32**, 360 (2015).
30 Y. Fu, S. Yang, B. Liu, E. Xia, and D. Huang, Multi-UAV cooperative trajectory planning based on the modified cheetah optimization algorithm, Entropy **25**, 1277 (2023).
31 Q. Shen, D. Zhang, M. Xie, and Q. He, Multi-strategy enhanced Dung Beetle optimizer and its application in three-dimensional UAV path planning, Symmetry **15**, 1432 (2023).
32 J. Xue, and B. Shen, Dung beetle optimizer: a new meta-heuristic algorithm for global optimization, J. Supercomput. **79**, 7305 (2023).
33 X. Zhao, Z. Zhao, Q. Wei, and C. Su, Dynamic analysis and trajectory solution of multi-robot coordinated towing system, J. Shanghai Jiaotong Univ. (Sci.) (2023), doi: 10.1007/s12204-023-2649-0.
34 Z. G. Zhao, X. T. Zhao, and C. Su, Dynamic modeling and simulation of a floating multi-robot coordinated towing system, J. Harbin Eng. Univ. **44**, 1825 (2023).
35 X. Wang, J. Guo, and Q. Tian, A forward-inverse dynamics modeling framework for human musculoskeletal multibody system, Acta Mech. Sin. **38**, 522140 (2022).
36 Z. G. Zhao, X.T. Zhao, and Q. Z. Wei, Trajectory planning for multi-robot coordinated towing system based on stability, High Tech. Lett. **30**, 43 (2024).
37 Y. Z. Zhou, Y. G. He, and Z. K. Xing, Power transformer vibration signal prediction based on IDBO-ARIMA, J. Electron. Meas. Instrum. **37**, 11 (2023).
38 Y. S. Yen, H. C. Chang, R. S. Chang, and H. C. Chao, Routing with adaptive path and limited flooding for mobile ad hoc networks, Comput. Electrical Eng. **36**, 280 (2010).
39 S. Mirjalili, SCA: A Sine Cosine Algorithm for solving optimization problems, Knowledge-Based Syst. **96**, 120 (2016).
40 X. Zhang, Y. Xu, C. Yu, A. A. Heidari, S. Li, H. Chen, and C. Li, Gaussian mutational chaotic fruit fly-built optimization and feature selection, Expert Syst. Appl. **141**, 112976 (2020).
41 Z. G. Zhao, Y. L. Wang, and J. S. Li, Appraise of dynamical stability of multi-robots cooperatively suspension system based on hybrid force-position-pose approach, J. Harbin Eng. Univ. **39**, 148 (2018).
42 Y. Z. Guan, W. X. Liu, and N. Yan, Research on cooperative motion planning of space multi-robots, J. Mech. Eng. **12**, 37 (2019).
43 Z. G. Zhao, F. J. Teng, G. T. Shi, Analysis and calculation on the feasible area of multi-robot combined lifting system, J. Shanghai Jiaotong Univ. **49**, 1174 (2015).
44 M. D. Phung, and Q. P. Ha, Safety-enhanced UAV path planning with spherical vector-based particle swarm optimization, Appl. Soft Comput. **107**, 107376 (2021).

45 Y. V. Pehlivanoglu, and P. Pehlivanoglu, An enhanced genetic algorithm for path planning of autonomous UAV in target coverage problems, Appl. Soft Comput. **112**, 107796 (2021).
46 Z. Pan, S. Yin, G. Wen, and Z. Tan, Reinforcement learning control for a three-link biped robot with energy-efficient periodic gaits, Acta Mech. Sin. **39**, 522304 (2023).
47 X. Huang, Opponent cart-pole dynamics for reinforcement learning of competing agents, Acta Mech. Sin. **38**, 521540 (2022).

基于力-位协同优化的多机悬吊系统有效避障规划

赵祥堂, 赵志刚, 苏程, 孟佳东, 桑虎堂

摘要 为了避免被吊运物、绳索、吊运机器人与环境中障碍物之间的碰撞, 基于力和位置协同优化方法研究了多机器人悬吊系统的避障规划. 在对系统运动学和动力学分析的基础上, 采用最小方差法求解系统的运动学和动力学逆解. 在求解的无碰撞可行空间中, 采用稳定蜣螂优化(SDBO)算法进行避障规划, 保证被吊运物稳定移动到工作空间中的目标点. 采用力-位协同优化方法对吊运机器人和绳索进行规划, 可以准确获得多机悬吊系统的最优避障轨迹. 最后, 通过仿真验证了该避障规划方法的正确性. 以一个特殊场景为例, 结果表明: SDBO算法优于蜣螂优化算法, 被吊运物规划轨迹长度减少14.51%, 高度减少79.88%, 最小适应度降低95.84%, 平均适应度降低94.77%. 研究结果有助于多机悬吊系统安全稳定地完成各种吊运任务, 并扩展了相关的规划和控制理论.